Available online at www.sciencedirect.com
SCIENCE DIRECT®
Dyes and Pigments 56 (2003) 151–157
DYES and PIGMENTS
www.elsevier.com/locate/dyepig

Structural influences on the photoelectric properties of TiO_2

C. Damm[a,*], F.W. Müller[a], G. Israel[a], S. Gablenz[b], H.P. Abicht[b]

[a]*Martin-Luther Universität Halle Wittenberg, Institut für Organische Chemie, Geusaer Str. 88, 06217 Merseburg, Germany*
[b]*Institut für Anorganische Chemie, Kurt-Mothes Str. 2, 06120 Halle/Saale, Germany*

Received 10 June 2002; received in revised form 28 August 2002; accepted 26 September 2002

Abstract

The Influence of crystal structure and surface coating on the photoelectric properties of TiO_2 pigments was studied using the transient photo-EMF. Amorphous TiO_2 did not show any photo-EMF signal showing that it is not a photoconductor. The crystalline TiO_2 modifications, anatase and rutile, behave like *n*-type photoconductors. In comparison to rutile, the maximum photo-EMF of anatase was significantly larger. While the photo-EMF signal of the rutile changed under repetitive laser flash exposure, the signal of anatase did not depend on number of flashes. This shows that only rutile contains a small amount of very deep traps. So in rutile a small part of charge carriers live longer than in anatase. Coating anatase with the photoelectrically inert $Ba(OH)_2{*}nH_2O$ or $BaCO_3$ reduced the photo-EMF signal. The epitaxial coating of rutile with SiO_2 and Al_2O_3 resulted in a complex photo-EMF signal that displayed two negative maximum voltages. Such behaviour suggests that heterojunctions may exist in the substrate.

Keywords: Photo-EMF; TiO_2; Structure; Coating

1. Introduction

TiO_2 is used in photovoltaic cells [1–8] and as a photocatalyst for the degradation of water pollutants [9–18]; both applications require the efficient photogeneration of charge in the TiO_2 particles.

The synthetic route and the prehistory of any TiO_2 pigment may determine its photoelectric properties and its suitability for photoelectric applications. That is due to differences in the structure of the pigments.

The aim of this work was to determine the influence of the crystal structure and surface coating of TiO_2 pigments on their photoelectric properties. For this transient photo-EMF (PEMF) studies were carried out.

In contrast to time of flight measurements or photovoltaic investigations [19–21] PEMF does not require contact between the sample and the electrodes and works without any external electric field. The method, which is well established for inorganic [10] and for organic photoconductors [22], characterizes the natural behaviour of photogenerated charge carriers.

Fig. 1 shows the principle of PEMF generation. After flash illumination, the gradient of the light absorption creates a concentration gradient of

* Corresponding author. Tel.: +49-3461-46-2062; fax: +49-3461-46-2158.
E-mail address: damm@chemie.uni-halle.de (C. Damm); israel@chemie.uni-halle.de (G. Israel).

0143-7208/03/$ - see front matter © 2002 Published by Elsevier Science Ltd.
PII: S0143-7208(02)00114-6

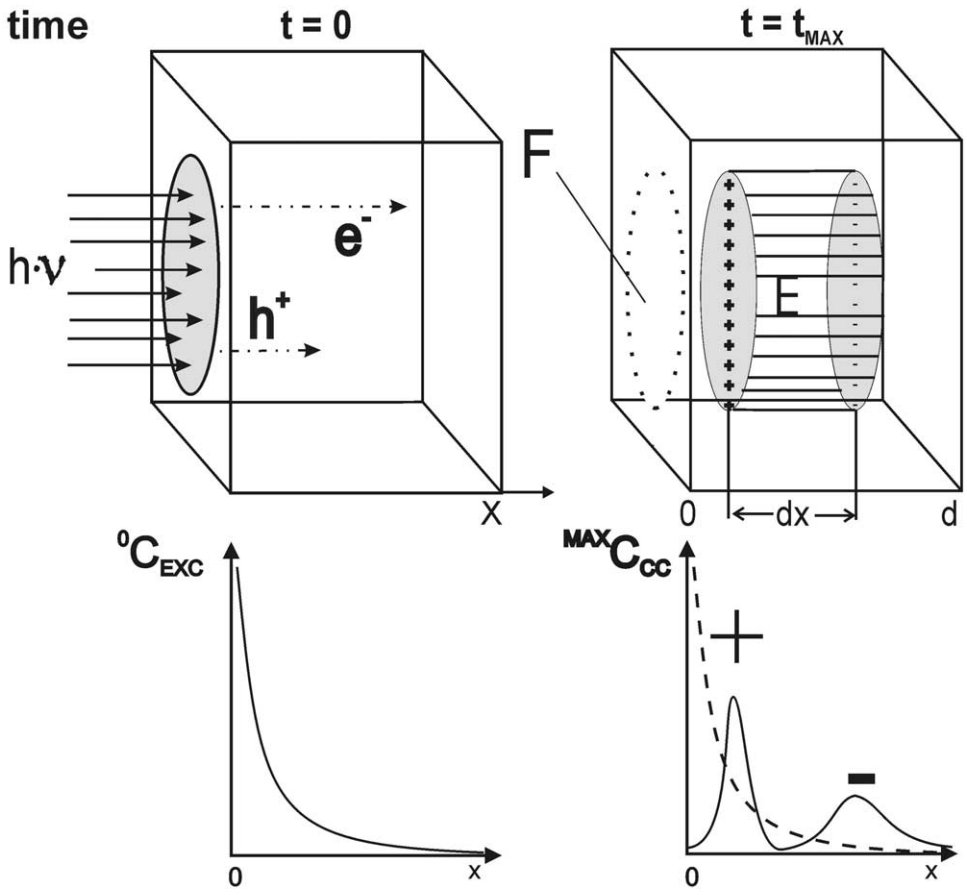

Fig. 1. Principle of the transient PEMF generation represented by a *n*-type photoconductor single crystal ($\mu_e > \mu_h$). $^{\circ}C_{EXC}$: charge carrier distribution immediately after the flash (at $t = 0$), $\vec{\mathbf{E}}$: internal electric field, dx: distance between the charge centres; $^{MAX}C_{CC}$: charge carrier distribution at the beginning of the decay process at $t = t_{MAX}$, here should be $U \cong U_{MAX}$.

electron hole pairs. The gradient represents the driving force for the diffusion of the charge carriers into the bulk material. An internal electric field arises due to the different mobilities of the electrons and holes ($\mu_h \neq \mu_e$), which can be measured externally as a transient photo-electromotive force (PEMF) or *Dember* voltage [23]. The type of photoconduction (*n*- or *p*-type) may be deduced from the sign of the PEMF.

1.1. PEMF kinetics

PEMF decay is caused by charge carrier recombination. Many photoconductors show PEMF signals having a crossing point within the decay process. Common kinetics does not correspond to such traces and so a biexponential rate law with two different partial PEMFs U_1^0 and U_2^0 [Eq. (1)] is used to describe all types of PEMF signals [22]:

$$U(t) = U_1^0 \cdot \exp(-k_1 t) + U_2^0 \cdot \exp(-k_2 t) \quad (1)$$

$$U_{MAX} = U_1^0 + U_2^0 \quad (2)$$

The process with the higher decay constant ($k_1 > k_2$) is referred to a "1" (parameters U_1^0, k_1), the PEMF maximum U_{MAX} should be the sum of both partial PEMF's U_1^0 and U_2^0 [see Eq. (2)].

The biexponential decay behaviour of the PEMF may be determined by different photoelectric

properties of the subsurface region and the bulk of a given substrate [22]. In this way, the PEMF rate constants, k_1 and k_2, should respond to each change of charge carrier concentration both in the subsurface and in the bulk of a given photoconductor. It has been shown [22] that k_1 may be assigned to a PEMF in the subsurface region of a photoconductor.

2. Experimental

2.1. Preparation of TiO_2 pigments

Amorphous TiO_2 was prepared by the spray hydrolysis of titanium tetraisopropoxide [24]. It was converted into the anatase and rutile forms by heating to 600 and 1100 °C, respectively.

The two crystal modifications were confirmed by X-ray diffraction: then, as prepared, amorphous TiO_2 does not show any diffraction pattern whereas the product heated to 600 °C shows a diffraction peak at $2\theta = 25.33°$ which is characteristic for anatase. Heating to 1100 °C leads to a diffraction peak at $2\theta = 27.42°$ which is typical for rutile [24].

The anatase was coated with $Ba(OH)_2{*}nH_2O$ as well as with $BaCO_3$ according to the method described in [25].

Rutile pigment which had been epitaxial coated with Al_2O_3 and SiO_2 was purchased from Kronos.

2.2. Sample preparation for PEMF measurements

PEMF measurements were carried out on pigment polymer dispersion films using polyvinyl butyrale (PVB) as binder. One-hundred milligrams of pigment were mixed with 3 g of a solution of PVB (10%) in 1,2-Dichlorethane. The mixture has been treated by ultrasound "Sonorex TK 52 H" (Bandelin, Germany) for 30 min. A glass plate ($A = 27$ cm^2) was coated with the resulting pigment dispersion. After air drying the layer was removed from the glass support. The layers had a thickness of 60–80 μm and total absorbancy in UV range. More details about the preparation of the dispersion films are given elsewhere [22].

2.3. PEMF device

The PEMF device is constructed like a capacitor with the sample as dielectric. Insulating foils between sample and electrodes prevent any galvanic contact. No charge injection occurs from the electrodes into the sample. In all cases, the PEMF measurements were carried out without any external electric field and so the natural behaviour of the charge carriers was measured. Details about the device and the PEMF-measurement procedure are described elsewhere [22]. Flash illumination was carried out using a nitrogen laser "PNL 100" (LTB, Germany) at a wavelength of 337 nm (about 3×10^{13} quanta per flash). All PEMF measurements were carried out under air at normal pressure and at 25 °C.

3. Results and discussion

3.1. Influence of crystal structure

Fig. 2(a and b) show the PEMF signals of TiO_2 samples having different crystal structures, Fig. 2(a) shows the PEMF generation and Fig. 2b the PEMF decay. The parameters of the PEMF decay are summarized in Table 1.

The results shown in Fig. 2(a and b) and Table 1 reveal that: amorphous TiO_2 does not show any PEMF showing that it is no photoconductor. Anatase and rutile display PEMF signals which are initially positive (see Fig. 2b), such signals being typical of *n*-type photoconductors. In the case of anatase, the value of U_{MAX} was three times higher than that of rutile. This means that in anatase the efficiency of charge separation under flash illumination is much higher than in rutile.

3.2. Sampling effects

The PEMF signals discussed above are the results of a single flash excitation. The influence of repeated illumination on PEMF generation (sampling effects) was determined using a time distance between two flashes of 120 s.

Fig. 3(a and b) show: that the PEMF of anatase was independent on the number of flashes and the

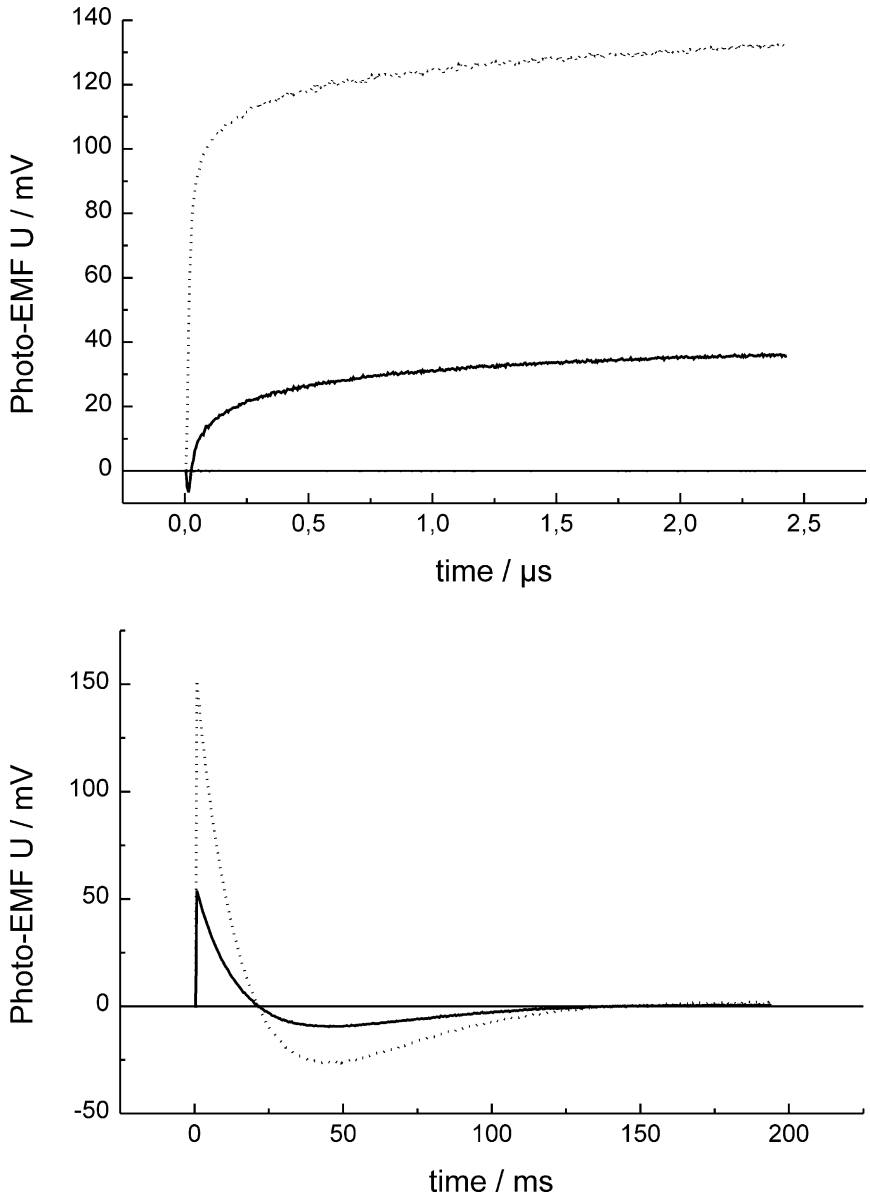

Fig. 2. (a) PEMF generation process in TiO_2 samples having different crystal structures, dashed line: anatase, solid line: rutile, line at zero potential: amorphous TiO_2. (b) PEMF decay process in TiO_2 samples having different crystal structures, dashed line: anatase, solid line: rutile, line at zero potential: amorphous TiO_2.

positive PEMF of rutile decreases with increasing flash number. After the 10th flash a signal with a negative sign was observed.

According to the trap concept [26] these results may be explained as follows. In the case of anatase, all photogenerated charge carriers were annihilated by recombination within 120 s after the flash. Thus, in the traps, there are no residual charges during the subsequent flash. In contrast to anatase, rutile seems to contain a small amount of very deep traps, so that in rutile some charges live longer than 120 s. The charge carriers remaining

Table 1
Influence of crystal structure on maximum voltage U_{MAX} and on the PEMF decay parameters of TiO_2 pigments

Structure	U_{max} (mV)	U_1^0 (V)	U_2^0 (V)	k_1 (s^{-1})	k_2 (s^{-1})
Amorphous	0	0	0	–	–
Anatase	152.0±2.1	9.473±0.027	−9.321±0.026	43.6±0.2	42.8±0.1
Rutile	54.0±0.4	5.696±2.374	−5.642±2.374	43.0±0.7	42.6±0.5

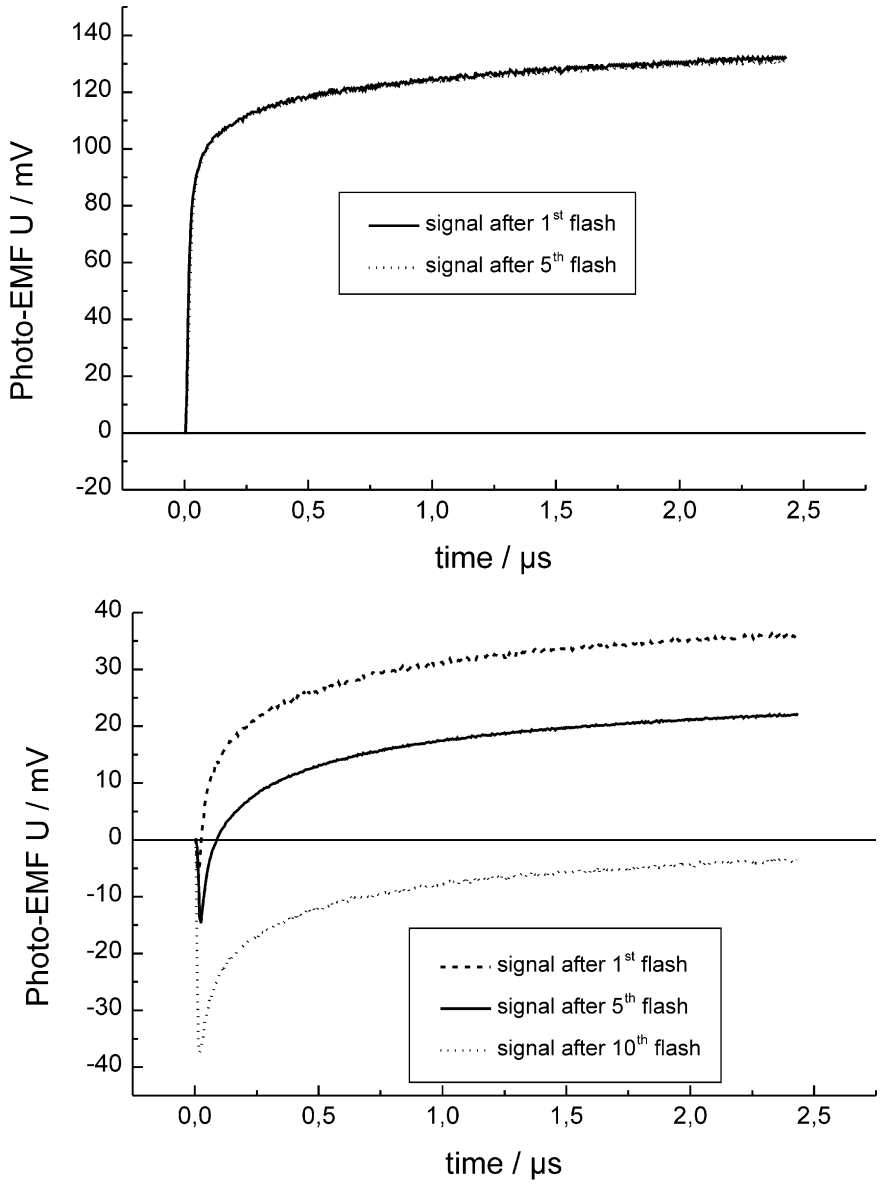

Fig. 3. (a) PEMF generation in anatase in dependence on number of laser flashes. (b) PEMF generation in rutile in dependence on number of laser flashes.

in deep traps may influence the diffusion of the charge carriers generated by the subsequent flash. This results in changes both in the form and the size of the PEMF signal.

3.3. Influence of surface coating

Table 2 shows the parameters of the PEMF decay of coated anatase samples in comparison to an uncoated one.

The coating of anatase with $Ba(OH)_2{*}nH_2O$ resulted in a strong reduction in the maximum PEMF U_{MAX}, also the rate constant k_1 increased strongly. Anatase coated with $BaCO_3$ showed no PEMF although the thicknesses of the $Ba(OH)_2{*}nH_2O$ and $BaCO_3$ layers was nearly the same [25].

Pure $Ba(OH)_2{*}nH_2O$ or $BaCO_3$ do not show any PEMF signal under comparable conditions [25], because they are photoelectric inert compounds.

The Ba-compounds in the core–shell-systems reduce the PEMF of anatase because they absorb the exciting light. In comparison to $Ba(OH)_2{*}nH_2O$, the $BaCO_3$ should absorb radiation of 337 nm more strongly, resulting in the completely disappearence of the PEMF of anatase.

The marked increase of the decay constant k_1, due to coating with $Ba(OH)_2{*}nH_2O$, shows that the surface recombination rate increases. The reason for this may be a change in the surface potential of anatase.

Fig. 4 shows the PEMF signal of rutile epitaxial coated with Al_2O_3 and SiO_2. The signal depicted in Fig. 4 is complex in that it shows two maximum voltages each with a negative sign. Such kind of signal, which cannot be described by Eq. (1), hints

Table 2
Influence of coating with photoelectric inert Ba-compounds on the PEMF decay parameters of anatase

Coating	U_{max} (mV)	U_1^0 (V)	U_2^0 (V)	k_1 (s^{-1})	k_2 (s^{-1})
Nil	152.0±2.1	9.473±0.027	−9.321±0.026	43.6±0.2	42.8±0.1
$BaCO_3$	0	0	0	–	–
$Ba(OH)_2{*}nH_2O$	10.6±2.3	$(1.21\pm0.13)\times10^{-2}$	$(-3.08\pm0.32)\times10^{-3}$	128.6±6.4	27.8±1.4

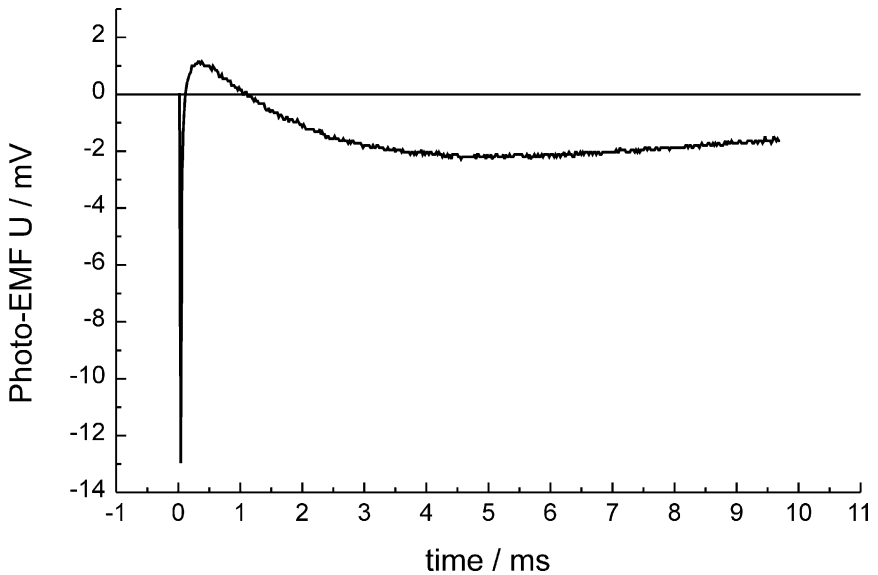

Fig. 4. PEMF signal of a rutile pigment epitaxial coated with Al_2O_3 and SiO_2.

at the presence of heterojunctions within the sample. As a consequence, space charges within the sample due to strong differences in the photoelectric properties of core and shell regions may influence the diffusion of photogenerated charge carriers. Further investigation of these phenomena is in progress.

4. Conclusions

The PEMF parameters of TiO_2 pigments may be affected by changes in the crystal structure or surface coating:

Amorphous TiO_2 does not show any PEMF signal, anatase and rutile behave like *n*-type photoconductors. In anatase, charge separation is more effective in comparison to rutile, so that anatase pigments show a higher photocatalytic activity than rutile.

Coating anatase with photoelectric inert Ba-compounds reduce the PEMF due to absorption of the exciting light by the Ba-compounds. Thus, the photocatalytic activity of anatase may be suppressed by coating.

Rutile pigment which has been epitaxial coated with Al_2O_3 and SiO_2 shows a complex PEMF transient that suggests the presence of heterojunctions in the substrate.

The results show that the PEMF method is able to detect structural influences on the photoelectric properties of pigments proving that it should be well suited for the characterization of TiO_2 pigments with respect to their application as photocatalysts or in solar cells.

Acknowledgements

This work was supported by the Kultusministerium Sachsen-Anhalt.

References

[1] O'Regan B, Grätzel M. Nature 1991;353:737.
[2] Hagfeld A, Grätzel M. Chem Rev 1995;95:49.
[3] Haque SA, Tachibana Y, Willis RL, Moser JE, Grätzel M, Klug DR, et al. J Phys Chem 2000;B104:538.
[4] Matsumoto M, et al. Solid State Ionics 1996;89:263.
[5] Sayama K, Suginao M, Sugihara H, Abe Y, Arakawa H. Chem Lett 1998:753.
[6] Hara K, Sayama K, Arakawa H, et al. Solar Energy Materials and Solar Cells 2000;64:115.
[7] Sayama K, Hara K, Tsukagoshi S, Suga S, Arakawa H, et al. Chem Commun 2000:1173.
[8] Hara K, Sayama K, Ohga Y, Shinpo A, Suga S, Arakawa H. Chem Commun 2001:569.
[9] Chun Hu, Yichong Wang, Hongxiao Tang. Chemosphere 2000;41(8):1205.
[10] (a) Paulus C, Wilke K, Breuer HD. J Inf Recording 1998; 24:299;
(b) Wilke K, Breuer HD. J Inf Recording 1998;24:309;
(c) Wilke K, Breuer HD. Photochem Photobiol 1999; A121:49.
[11] Morrison C, Bandara J, Kiuri J. J Adv Oxid Technol 1996;1(2):160.
[12] Pelizzetti E, Minero C, Tinucci L, Serpone N. Langmuir 1993;9:2995.
[13] Bahnemann DW. Isr J Chem 1993;33:115.
[14] Zi-Shen Guan, et al. J Mater Res 2001;16(4):907.
[15] Shengping Ruan, et al. Mat Chem Phys 2001;69:7.
[16] Piscopo A, Robert D, Weber JV. Photochem Photobiol 2001;A139:253.
[17] Jiaguo Yu, et al. Mat Chem Phys 2001;69:25.
[18] Laubrich J, Israel G. J Inf Recording 1998;24:427.
[19] Kallmann H, Pope M. J Chem Phys 1959;30:585.
[20] Bonham JS. Australian J Chem 1976;29:2123.
[21] Pope M, Swenberg CE. Electronic processes in organic crystals and polymers. Oxford: Oxford University Press; 1999.
[22] (a) Israel G, Müller FW, Damm C, Harenburg J. J. Inf. Recording 1997;23:559;
(b) Damm C, Müller FW, Israel G. J. Inf. Recording 2000;25:553;
(c) Müller FW, Damm C, Israel G. J. Inf. Recording 2000;25:611.
[23] Dember H. Phys Z 1931;32:554–856;
Dember H. Phys Z 1932;33:207.
[24] Gablenz S, Völtzke D, Abicht H-P, Neumann-Zdralek J. J Mat Sci Lett 1998;17:537.
[25] Gablenz S, Damm C, Müller FW, Israel G, Rössel M, Röder A, et al. Solid State Sciences 2001;3:291.
[26] Hamann C, Heim J, Burghardt H. Organische leiter, halbleiter und photoleiter. Berlin: Akademie-Verlag; 1980.